Journal of Water & Health

Journal of Water and Health Vol 21 No 10, 1503 doi: 10.2166/wh.2023.149

Temporal and spatial variations of disinfection by-products in South Taihu's drinking water, Zhejiang Province, China

Tao Liu[a], Min Zhang[b], Dong Wen[a], Yun Fu[a], Jianhua Yao[a], Guojian Shao[a] and Zhang Peng[a,*]

[a] Huzhou Center for Disease Control and Prevention, Huzhou, Zhejiang Province 313000, China
[b] Hunan Provincial Center for Disease Control and Prevention, Changsha, Hunan Province 410005, China
*Corresponding author. E-mail: hzjkzp@163.com

ZP, 0000-0003-2540-8515

ABSTRACT

Some disinfection by-products (DBPs) in drinking water present a potential safety concern. This study focuses on the elements influencing DBPs formation. A total of 120 water samples were collected from 10 different drinking water facilities spanning 5 counties within Huzhou, Zhejiang Province, China. Concentrations of trihalomethanes (THMs) and haloacetic acids (HAAs) were observed to be 14.5 and 27.4 μg/L, respectively, constituting 34 and 64% of the total DBPs. Seasonal fluctuations demonstrated that HAAs, THMs, halonitromethanes (HNMs), and haloacetonitriles (HANs) followed a similar pattern with higher levels in summer or autumn compared to spring. Importantly, the concentrations of HAAs and THMs were markedly higher in Taihu-sourced water compared to other sources. Geographically, Nanxun exhibited the highest levels of total DBPs, HAAs, and THMs, while Deqing and Changxing demonstrated significantly lower levels. Correlation studies between water quality parameters and DBPs revealed that factors such as chloride content, temperature, and residual chlorine positively influenced DBPs formation, whereas turbidity negatively affected it. Principal component analysis suggested similar formation processes for HANs, haloketones (HKs), HNMs, and THMs. Factors such as temperature, chemical oxygen demand (COD), and residual chlorine were identified as significant contributors to the prevalence of HAAs.

Key words: DBPs, drinking water, influencing factors, Taihu

HIGHLIGHTS

- Twenty classes of DBPs and eight kinds of water quality parameters were monitored.
- The impacts of water source and season were different between DBP species.
- The temperature and COD played important roles in HAAs occurrence.

GRAPHICAL ABSTRACT

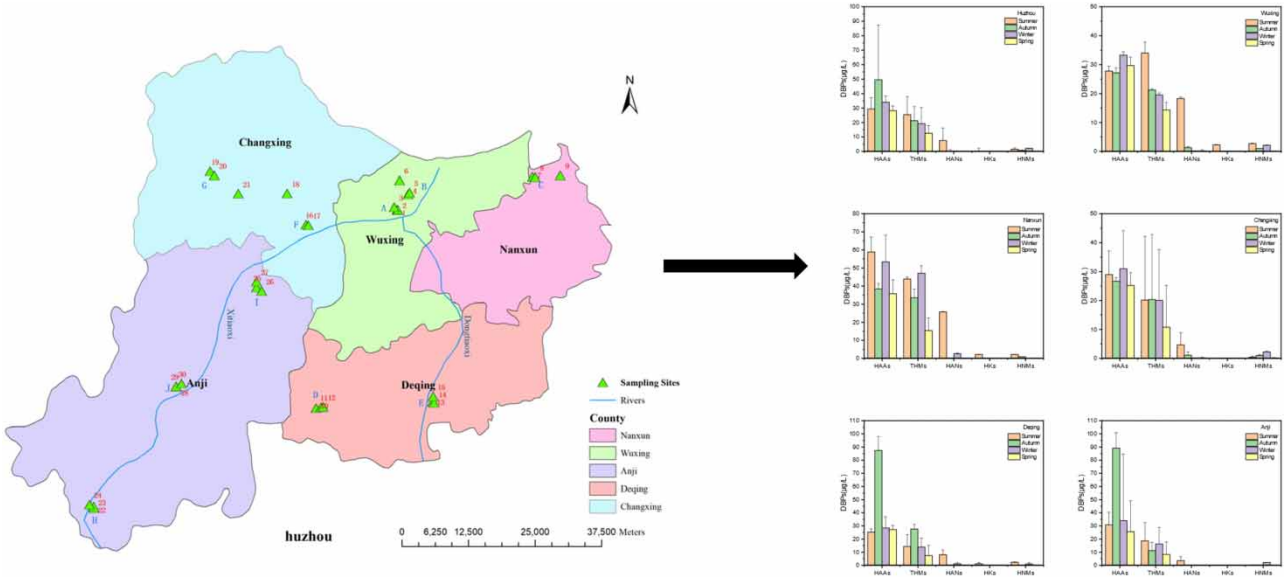

1. INTRODUCTION

Chemical disinfectants like free chlorine and chlorine dioxide are commonly applied in drinking water distribution systems due to their cost-effectiveness and efficiency in eliminating microorganisms, thereby enhancing water quality and public health (Benson *et al.* 2017). However, the formation of harmful disinfection by-products (DBPs), which are produced by the interaction of disinfectants with various inorganic and organic substances (e.g., bromide, humic substances, amino acids, and environmental pollutants) (Yang & Zhang 2016; Jiang *et al.* 2020) untreated water, has raised concerns (Korotta-Gamage & Sathasivan 2017). Numerous studies have documented the correlation between prolonged exposure to DBPs via ingestion, inhalation, and dermal pathways (Kumari *et al.* 2015; Wang *et al.* 2019; Ates *et al.* 2020) and their toxic synergistic impacts on genes, cells, endocrine systems, fetuses, and cancer in animals (Hrudey *et al.* 2015; Kolb *et al.* 2017).

Trihalomethanes (THMs) and haloacetic acids (HAAs) are among the most frequently detected classes of DBPs, originating from the chlorination process of drinking water supplies (Hao *et al.* 2017). Regulatory bodies such as the United States Environmental Protection Agency (USEPA), the European Community, and the World Health Organization (WHO) recommend respective THMs concentrations of 80 μg/L, 100 μg/L, and [TTHMs/WHO guideline value] ≤ 1 in drinking water (WHO 2004; USEPA 2010). In China, the prescribed concentrations for bromodichloromethane (BDCM), dibromochloromethane (DBCM), tribromomethane (TBM), dichloroacetic acid (DCAA), and trichloroacetic acid (TCAA) are 60, 100, 100, 50, 100 μg/L, respectively, and [TTHMs/respective guideline value] ≤ 1 (MOH 2006). Emerging DBPs such as haloacetonitriles (HANs), haloketones (HKs), halonitromethanes (HNMs), and iodine-DBPs have recently gained attention due to their higher cellular cytotoxicity and genotoxicity than traditional c-DBPs (Jeong *et al.* 2015; Mao *et al.* 2016). Additionally, factors including water sources, treatment processes, pipe materials, hydraulic conditions, and sediments on pipe walls contribute to the occurrence of DBPs in different drinking water systems (Abbas *et al.* 2014; Kali *et al.* 2021).

Huzhou City, located in the northern part of Zhejiang Province on China's eastern coast, spans an area of 5,818 km^2 and is home to approximately 2.67 million people. The region's mild temperature and subtropical monsoon climate result in four distinct seasons. Primary surface water sources include Taihu Lake, reservoirs, and the Tiaoxi river. Taihu Lake, one of the five largest freshwater lakes in China, lies downstream of the Tiaoxi river. Over recent decades, population growth and industrial development have led to substantial sewage discharge into rivers and lakes, causing significant ecological and watershed damage (Hong *et al.* 2015; Wu *et al.* 2020).

The objectives of this study are (i) to examine the spatial and temporal variations of DBPs in 10 full-scale drinking water systems that employ the chlorine sequential disinfection method in their drinking water treatment plants (DWTPs); (ii) to

identify contributing factors (e.g., water quality, operational parameters) to these variations; and (iii) to explore the relationships between different DBP levels to predict future haloacetonitrile (HAL) occurrences.

2. MATERIAL AND METHODS

2.1. Site selection and sampling

Accounting for variables such as the type of water source, treatment processes, population served, and geographical distribution, we conducted a survey across 10 DWTPs in 5 counties of Huzhou. For each monitoring point per season, we collected a sample of source water, finished water, and tap water from the end of the distribution network. The sample collection was scheduled as follows: May 2019, August 2019, November 2019, and January 2020. Over the four seasons, we collected a total of 120 water samples – 30 samples each season, with 80 samples obtained from the finished water and tap water at the terminal of the distribution network, as presented in Table 1 and Figure 1.

The DWTPs primarily relied on surface water sources, and chlorine-based disinfectants were employed for water disinfection. The investigated finished or tap water samples were treated using traditional techniques, including coagulation, sedimentation, filtration, and chlorination. Depending on the raw water sources at the DWTPs, we divided the 10 DWTPs into 4 water distribution systems: 2 sourced from reservoir water mixed with river water, 3 from reservoir water systems, 4 from the Tiaoxi water system, and 1 from the Taihu Lake water system.

The collection of the 120 samples followed the GB/T 5750-2006 guidelines. Prior to sampling, we allowed the water at each sampling point to stand for 10–30 min. We then filled one 5 L plastic container, one 2.5 L plastic container, and one 1,000 mL amber glass sample bottle, ensuring the glass bottle was filled to capacity without air gaps. After sample collection, we labeled the respective bottles with pertinent information including the water plant's name, sample type (source water, treated water, distribution endpoint water), collection time, and sample number. All samples were maintained at low temperatures (4 °C) and stored in light-protected conditions before being transported to the Huzhou Municipal Center for Disease Control and Prevention (CDC) laboratory for testing within 4 h.

2.2. Chemical and reagent preparation

An Agilent 7890B capillary gas chromatograph and an electron capture detector were purchased from Agilent Corporation (USA). Ultrapure water was produced using a Milli-Q ultrapure grade purification system (Millipore Corporation, USA). Other chemicals were of analytical reagent grade and were obtained from Sinopharm Chemical Reagent Co. Ltd (China). Standard solutions of chloroform (TCM), dichlorobromo-methane (DCBM), chlorodibromo-methane (DBCM), tribromomethane (TBM), dichloroacetonitrile (DCAN), trichloroacetonitrile (TCAN), chlorobromo-acetonitrile (BCAN), dibromoacetonitrile (DBAN), 1,1-dichloroacetone (1,1-dichloro-2-propanone, DCP), 1,1,1-trichloroacetone (1,1,1-trichlo-2-propanone, TCP), and trichloronitromethane (TCNM) were purchased from Accustandard.

Table 1 | Basic information of DWTPs monitoring points

DWTPs	Water source	Type of water source	Treatment processes	Actual water supply capacity (tons/day)	Samper number
A	Reservoir water + Tiaoxi	Mixed water	Liquid Chlorine	100,000	1, 2, 3
B	Reservoir water + Rivers	Mixed water	Liquid Chlorine	200,000	4, 5, 6
C	Taihu water	Taihu water	Liquid Chlorine	72,000	7, 8, 9
D	Dongtiaoxi	Rivers	Bleaching Powder	1,200	10, 11, 12
E	Reservoir water	Reservoir water	Liquid Chlorine	100,000	13, 14, 15
F	Xitiaoxi	Rivers	Liquid Chlorine	9,000	16, 17, 18
G	Reservoir water	Reservoir water	Chlorine Dioxide Compound	5,000	19, 20, 21
H	Xitiaoxi	Rivers	Bleaching Powder	300	22, 23, 24
I	Xitiaoxi	Rivers	Bleaching Powder	26,400	25, 26, 27
J	Reservoir water	Reservoir water	Liquid Chlorine	50,000	28, 29, 30

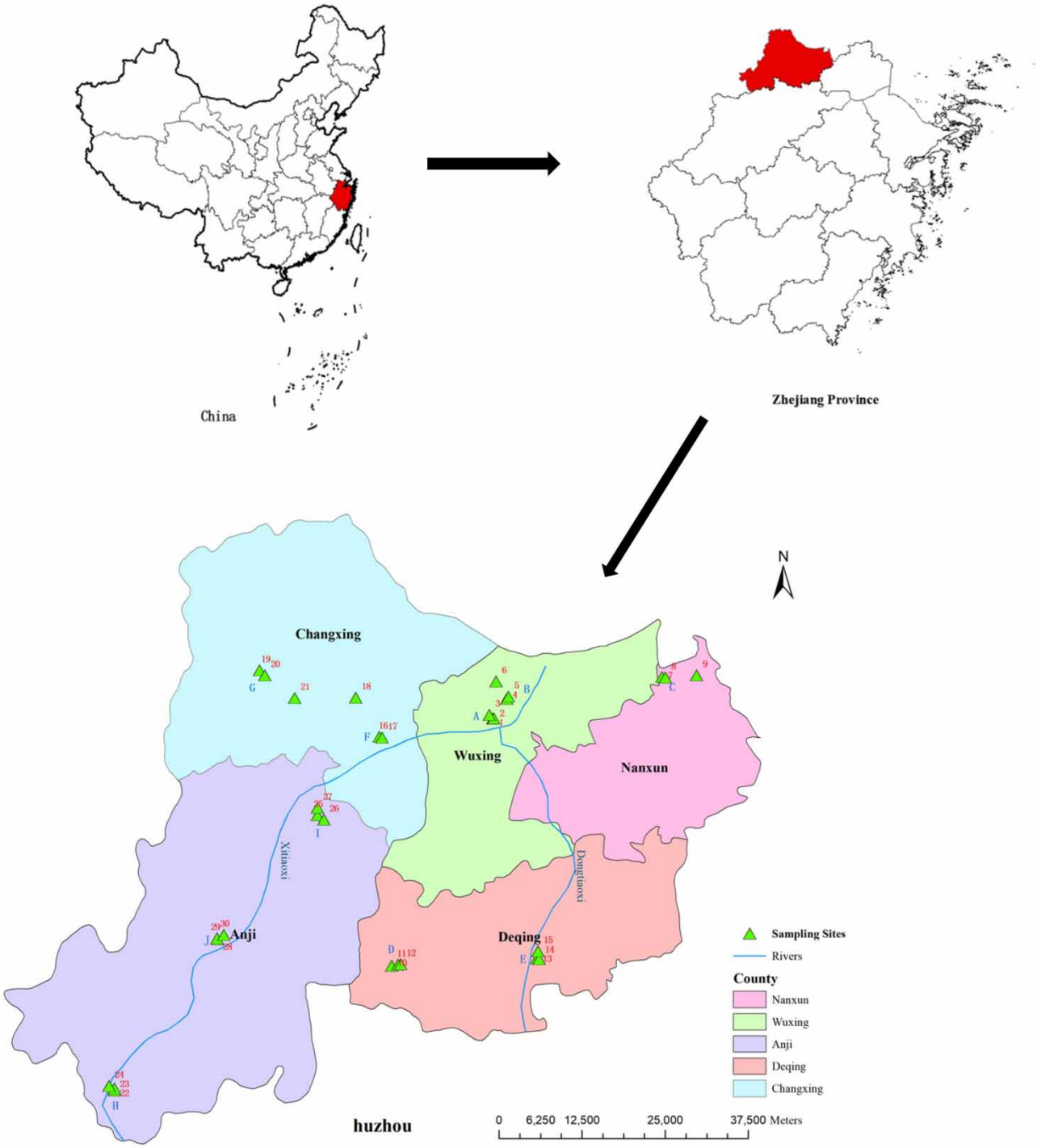

Figure 1 | Sampling sites in Huzhou Region.

2.3. Determination of DBPs

We commenced our experiment by utilizing a 1 L brown glass sampling bottle. Prior to sample collection, 1.0 g of ascorbic acid was added to the bottle to inhibit the chlorination reaction. Subsequently, we filled the bottle with water and sealed it.

For the analysis of trihalomethanes (THMs), haloacetonitriles (HANs), halogenated ketones (HKs), and trichloronitromethane (TCNM), we extracted a 10 mL water sample and directly placed it into a 20 mL headspace vial. We further

added 3 g of sodium chloride, sealed it immediately, and then shook the vial thoroughly. The sample was then analyzed using a headspace sampler-gas chromatograph as per the established conditions. The Agilent GC ChemStation was responsible for data acquisition, analysis, and subsequent result generation. The process involved using an HP-5 chromatographic column (30 m × 0.32 mm × 1.0 μm) and high-purity nitrogen (99.999%) served as the carrier gas. The temperature programming started at an initial 50 °C, maintained for 5 min, then gradually increased to 100 °C at a rate of 3 °C/min. Other specific parameters were set as follows: inlet temperature at 200 °C, electron capture detector temperature at 300 °C, a flow rate of 1.0 mL/min, and a split ratio of 50:1. The make-up gas flow was set at 30 mL/min. Heating box temperature: 70 °C, loop temperature: 80 °C, transfer line temperature: 90 °C; vial equilibration time: 20 min, pressure equilibration time: 0.1 min, injection time: 1 min; air filling pressure: 15 psi, filling flow: 50 mL/min, shake seven times, and vent after extraction. Injection volume: 1,000 μL.

THMs, HANs, HKs, and TCNM were executed using the headspace salt-assisted gas chromatography-electron capture detector (GC-ECD) method. Our quality control procedure was crafted to mitigate any potential interference from the pretreatment process on the target substance's determination. We incorporated a process blank experiment to certify the absence of such interference. Each batch of samples was subjected to a blank test using pure water instead of the actual test sample, and no disinfection by-products (DBPs) were detected. Post-verification, we confirmed the experimental process as contamination-free. To create a standard curve, we introduced a volume of mixed standard solution into the headspace bottle resulting in concentrations ranging from 1 to 50 μg/L. This demonstrated a robust linear relationship, with correlation coefficients exceeding 0.998. Utilizing a low-concentration sample spiked at 5 μg/L, we computed the method's detection limits at a signal-to-noise ratio three times. We attained a detection limit for TCAN as low as 0.005 μg/L, while the detection limit for DBAN, possessing the lowest sensitivity, could still reach up to 0.200 μg/L. With factory water as the substrate, the recovery rates and relative standard deviations (RSDs) at 5.0 μg/L spiking fluctuated between 70.62–118.53% and 2.10–8.62%, respectively.

In case of HAAs, we extracted 25 mL of the water sample to be tested directly into a 50 mL extraction bottle, added 2 mL of concentrated sulfuric acid, and mixed thoroughly. About 3 g of anhydrous copper sulfate was swiftly added, followed by approximately 10 g of anhydrous sodium sulfate, shook well. Then, 4.0 mL of methyl tert-butyl ether containing 300 μg/L internal standards (1,2-DBP) was added, shaken, and stood still for 5 min. We took 3.0 mL of the supernatant into another 16 mL derivatization bottle, added 1.0 mL of freshly prepared sulfuric acid-methanol solution, and derivatize it on a heating block at 50 °C for 120 min. Took out the derivatization bottle, added 4 mL of saturated sodium bicarbonate solution dropwise after cooling to room temperature, covered with a stopper, shook and kept deflating; finally, we took 1–1.5 mL of the supernatant into the extraction bottle, and added a small amount of anhydrous sodium sulfate, took 2 μL of supernatant for gas chromatography analysis, completed data acquisition and data analysis by AgilentGC chemical workstation and got the results directly. We used DB-5 ms chromatographic column (30 m × 0.32 mm × 0.25 μm), high-purity nitrogen (99.999%) as a carrier gas, program temperature: initial 50 °C for 7 min, increased to 70 °C at 4 °C/min, then 30 °C/min to 250 °C, and then held for 5 min. The inlet temperature was 200 °C, the electron capture detector temperature was 300 °C, the flow rate was 9.0 mL/min, and the split ratio was 3:1. The make-up gas flow was 30 mL/min.

To ensure quality and control for HAAs, we adopted process blank experiments to verify the absence of interference in the test process. This involved replacing the test samples with pure water in each batch for blank tests. The standard curve, developed from these results, displayed strong linearity, with correlation coefficients across all concentrations exceeding 0.998. The recovery rates for the seven haloacetic acids were as follows: monochloroacetic acid 104.14%, dichloroacetic acid 104.79%, trichloroacetic acid 120.68%, monobromoacetic acid 109.35%, tribromoacetic acid 69.49%, monochlorobromoacetic acid 108.37%, dibromochloroacetic acid 90.47%. For monobromoacetic acid and monobromodichloroacetic acid, due to the unavailability of standard reference materials, their spiked recovery rates were not determined.

2.4. Water quality analysis

Various water quality parameters were measured in a laboratory setting in accordance with the National Standard Methods (Standard Examination Methods for Drinking Water, GB/T 5,750, 2006, as specified by the Chinese Ministry of Health). These parameters include pH (measured with a pH meter), temperature (thermometer), residual chlorine (analyzed by the 3,3–5,5-tetramethylbenzidine colorimetry method), UVA254 (UV-visible spectrophotometry, Shimadzu UV-2450), Cl^-, and Br^- (ion chromatography, Dionex ICS-1500), along with turbidity (assessed using a turbidimeter, HACH 2100N).

2.5. Data analysis

We computed fundamental descriptive statistics for each individual variable. To identify seasonal differences in water quality parameters, we employed nonparametric hypothesis testing. Results that yielded two-tailed *p*-values of less than 0.05 were considered statistically significant. To explore the correlation between disinfection by-products (DBPs) and water quality parameters, we utilized both Spearman correlation analysis and principal component analysis. All statistical computations were conducted using SPSS software (Version 24).

3. RESULTS AND DISCUSSION

3.1. Water quality parameters

All collected data underwent a normality test and exhibited a skewed distribution. We utilized nonparametric analysis to perform comparisons between the datasets. Table 2 depicts the characteristics of water quality and operational parameters across different seasons in Huzhou City. Temperature, turbidity, and BOD all demonstrated significant seasonal variability ($p < 0.05$). The median turbidity level in drinking water exhibited a spring > winter > autumn > summer pattern, which might be attributed to rainfall carrying particulate matter into the source water. The warmer temperatures in summer and autumn compared to spring and winter could provide a more favorable environment for the growth of bacteria and other microorganisms, thereby contributing to an increase in COD by releasing organic matter into the source water (Fang *et al.* 2010; Ly *et al.* 2017). However, certain drinking water parameters, such as pH, Cl^-, Br^-, UVA_{254}, and residual chlorine, did not exhibit any seasonal changes, potentially indicating that water treatment technology was not season-dependent and that consistent methodology had been applied throughout the year.

As source water variation can influence water quality parameters, we analyzed these parameters across different source waters in Huzhou City, as detailed in Table 3. The analysis revealed that the pH of Taihu water is higher than that of other source waters. This could be linked to eutrophication in Taihu Lake, where algal blooms consume large amounts of CO_2 during photosynthesis, subsequently elevating the pH of Taihu water (Wu *et al.* 2018). Other water quality parameters remained unchanged across different source waters, suggesting that these parameters were largely consistent regardless of the water source.

3.2. Descriptive statistics of DBPs in Huzhou

Table 4 presents the concentrations of DBPs in the drinking water of Huzhou city. For the skewed distribution of the data results, we used median values to depict each compound's concentration. THMs and HAAs were the principal constituents of DBPs in all samples, accounting for 34 and 64% of all DBPs, respectively. Together, they represented approximately 98% of the total DBPs, which was higher than the levels found in the drinking water of Beijing city (Wei *et al.* 2010). The respective levels of THMs and HAAs in the Huzhou region were 14.5 and 27.4 μg/L, which were lower than those reported in Iran's Bushehr Province (Dobaradaran *et al.* 2020), China's Haihe River, and Nigeria (Benson *et al.* 2017), were higher than those found in Bohai Bay, China (Niu *et al.* 2017), and India's river water (Padhi *et al.* 2019). TCM was the dominant component of THMs, with a concentration of 11.35 μg/L. Among HAAs, TBAA and DBCAA had the highest mean levels, peaking at 60.60 and 82.57 μg/L, respectively. The concentrations of other DBPs such as HANs, HKs, and HNMs were considerably lower than those of THMs and HAAs. The elevated levels of THMs and HAAs, relative to other DBPs in Huzhou city, could be attributed to several factors: (1) The water in this study displayed higher levels of UVA_{254} and COD, indicating an elevated DOC level which usually leads to a high level of DBPs (Zhou *et al.* 2019). Additionally, the disinfection duration in the waterworks could affect the generation of DBPs (Mompremier *et al.* 2018). (2) Nine out of 10 water treatment plants utilized sodium hypochlorite for disinfection, with only one using ozone. Chlorine-based disinfection tends to produce higher levels of DBPs in water than ozone disinfection (Zheng *et al.* 2017).

3.3. Seasonal variations of DBPs from different water sources

The formation of all DBPs displayed a marked seasonal influence, as depicted in Figure 2. HAAs levels were significantly higher in winter than in spring and summer ($p < 0.05$), a seasonal variation pattern similar to that observed in Beijing's drinking water (Wei *et al.* 2010). This could be attributed to the rate of DBPs transformation – lower temperatures in winter could decelerate the transformation rate of HAAs, resulting in their elevated concentration during this season. THMs showed a distinct increase in both summer and autumn as compared to spring ($p < 0.05$), a finding consistent with certain studies indicating higher total THM levels in tap water during summer (Charisiadis *et al.* 2015). This elevation can be explained

Table 2 | Characteristics of water quality and operational parameters in different seasons of Huzhou City

	Spring					Summer					Autumn					Winter					
Parameters	**Mean**	**Max**	**Min**	**Median**	**Std**	**Mean**	**Max**	**Min**	**Median**	**Std**	**Mean**	**Max**	**Min**	**Median**	**Std**	**Mean**	**Max**	**Min**	**Median**	**Std**	***P***
UVA_{254}	0.02	0.04	0.01	0.02	0.01	0.02	0.09	0.01	0.01	0.02	0.02	0.09	0.01	0.02	0.02	0.02	0.03	0.01	0.02	0.01	0.08
pH	7.34	7.89	6.59	7.51	0.42	7.28	7.95	6.45	7.32	0.47	7.34	7.92	6.55	7.50	0.45	7.33	7.91	6.45	7.42	0.42	0.85
Turbidity	1.00	6.52	0.17	0.38	1.61	0.40	3.10	0.08	0.18	0.67	0.34	0.78	0.12	0.25	0.20	0.78	5.34	0.23	0.36	1.19	0.05
Cl^- (mg/L)	12.89	47.53	0.79	5.76	15.68	10.62	44.58	2.02	7.79	12.03	7.38	14.69	1.66	7.09	3.76	11.99	46.20	0.96	6.28	12.82	0.42
Br^- (mg/L)	0.24	0.32	0.06	0.25	0.05	0.25	0.25	0.25	0.25	0.00	0.25	0.25	0.25	0.25	0.00	0.25	0.25	0.25	0.25	0.00	0.39
COD (mg/L)	1.17	1.50	0.85	1.15	0.18	1.60	2.40	1.18	1.44	0.38	1.50	2.11	1.12	1.38	0.29	1.12	1.41	0.79	1.05	0.20	0.00
Residue Chlorine (mg/L)	0.26	0.60	0.02	0.21	0.17	0.26	0.60	0.00	0.20	0.20	0.35	0.84	0.02	0.36	0.21	0.32	0.80	0.02	0.31	0.21	0.33
Temp (°C)	7.85	10.80	6.00	7.75	1.20	23.59	26.60	21.60	23.45	1.29	24.35	28.40	20.50	24.50	1.90	13.54	16.40	11.80	13.50	1.16	0.00

Table 3 | Characteristics of water quality and operational parameters of different water sources of Huzhou City

	Mixed water					Taihu water					Rivers					Reservoir water					
Parameters	**Mean**	**Max**	**Min**	**Median**	**Std**	**Mean**	**Max**	**Min**	**Median**	**Std**	**Mean**	**Max**	**Min**	**Median**	**Std**	**Mean**	**Max**	**Min**	**Median**	**Std**	***P***
UVA_{254}	0.02	0.03	0.01	0.02	0.01	0.02	0.03	0.01	0.01	0.01	0.02	0.04	0.01	0.02	0.01	0.03	0.09	0.01	0.02	0.03	0.12
pH	6.68	6.98	6.45	6.66	0.17	7.71	7.80	7.62	7.71	0.06	7.48	7.95	6.71	7.58	0.38	7.41	7.76	7.13	7.41	0.20	0.00
Turbidity	0.39	2.17	0.11	0.26	0.49	0.27	0.54	0.11	0.24	0.13	1.05	6.52	0.13	0.46	1.58	0.34	0.87	0.08	0.29	0.21	0.10
Cl^- (mg/L)	6.80	11.61	1.20	6.27	3.41	34.77	47.53	2.94	44.47	19.61	7.18	26.92	0.79	6.17	5.52	10.03	36.09	2.13	6.39	9.49	0.51
Br^- (mg/L)	0.25	0.32	0.25	0.25	0.02	0.23	0.25	0.06	0.25	0.07	0.25	0.25	0.25	0.25	0.00	0.25	0.25	0.25	0.25	0.00	0.26
COD (mg/L)	1.19	1.44	0.92	1.22	0.15	1.32	1.71	0.99	1.25	0.28	1.42	2.40	0.79	1.36	0.42	1.37	2.06	0.88	1.35	0.30	0.05
Residue chlorine (mg/L)	0.36	0.70	0.10	0.35	0.20	0.39	0.80	0.10	0.30	0.25	0.27	0.84	0.00	0.21	0.20	0.26	0.52	0.02	0.28	0.17	0.94
Temp (°C)	16.41	26.60	6.40	17.00	6.82	16.59	23.10	7.90	17.40	6.79	17.64	27.60	6.40	19.30	7.44	17.77	28.40	6.00	19.20	7.37	1.00

Table 4 | The concentration of all DBPs of Huzhou City (μg/L)

Group	Compound	*N*	Mean	Std	Median	Min	Max
THMs	TCM	80	12.532	10.703	11.350	0.008	44.400
	DCBM	80	3.187	3.435	2.400	0.005	14.800
	DBCM	80	2.330	4.780	0.750	0.010	22.800
	TBM	80	0.923	2.813	0.025	0.025	14.800
HAAs	MCAA	80	1.871	1.522	1.735	0.350	6.990
	DCAA	80	3.080	1.440	2.820	1.250	8.830
	TCAA	80	3.950	1.600	3.480	2.050	10.270
	MBAA	80	3.170	5.550	0.500	0.500	26.400
	DMAA	80	3.590	0.790	3.240	2.500	6.830
	TBAA	80	8.200	12.960	3.300	0.100	60.600
	BCAA	80	4.150	2.230	4.070	0.250	17.200
	BDCAA	80	3.850	1.680	4.680	0.150	5.820
	DBCAA	80	8.275	15.703	3.535	0.150	82.570
HANs	TCAN	80	2.038	4.173	0.025	0.025	17.300
	DCAN	80	0.238	0.686	0.003	0.003	2.500
	BCAN	80	0.230	0.690	0.050	0.050	3.300
	DBAN	80	0.300	0.900	0.100	0.100	4.900
HKs	DCP	80	0.244	0.661	0.025	0.025	2.400
	TCP	80	0.027	0.020	0.025	0.025	0.200
HNMs	TCNM	80	0.936	1.151	0.350	0.005	5.900

by the fact that higher temperatures and chlorine residuals could potentially enhance the formation of THMs (Kali *et al.* 2021). HANs were significantly more abundant in summer than in other seasons ($p < 0.05$). In contrast, HNMs demonstrated considerably lower concentrations in spring as compared to other seasons ($p < 0.05$). The variation trends of HANs and HNMs were similar to those observed in Jinhua (Zhou *et al.* 2019). This pattern could be attributed to the increased algal blooms in summer, which could escalate the demand for Cl_2, subsequently promoting the formation of DBPs (Chowdhury 2018). However, the concentrations of HKs were below detection limits in most samples, thereby revealing no noticeable seasonal distribution in pairwise comparisons.

3.4. Water source variations of DBPs

The drinking water samples from Huzhou were categorized into four types: mixed water (comprising reservoir water combined with water from Dongtiaoxi or Xitiaoxi), Taihu water, river water (originating from Dongtiaoxi or Xitiaoxi), and reservoir water. The diverse array of DBPs within these water sources is presented in Figure 3. Both HAAs and THMs levels were found to be significantly higher in Taihu water than in mixed water, river water, and reservoir water ($p < 0.05$). The mixed water and river water flow into Taihu Lake, possibly introducing pollutants into it. Over recent years, Taihu Lake has experienced serious water pollution, characterized by a high concentration of organic matter, which could account for the elevated HAAs and THMs levels (Wu *et al.* 2018, 2020). Meanwhile, no noticeable differences were observed in the levels of HANs and HNMs in the drinking water, likely because they remained undetected in most of the water samples. The median concentration of HKs in different water sources stood at 0.05 μg/L, suggesting that most water samples showed no detectable presence of HKs.

3.5. Spatial distribution of DBPs concentration

Figure 4 displays the regional distribution of DBPs in Huzhou. The overall concentration of DBPs and HAAs was highest in Nanxun, followed by Anji, whereas the levels in Deqing and Changxing were significantly lower. The Nanxun sampling site's proximity to Taihu Lake could account for these higher levels, given its status as a source of Taihu water. In terms of spatial dispersion of THMs, Nanxun again recorded the highest levels, with Wuxing ranking next, and Deqing and Changxing registering lower levels. DCBM, DBCM, and TBM concentrations were highest in Nanxun, while the principal component TCM reached its peak in Wuxing. This disparity might be explained by the notably high median CL^- concentration in Nanxun water samples at 44.47 μg/L, with concentrations in other areas being lower. The formation of THMs and HAAs typically

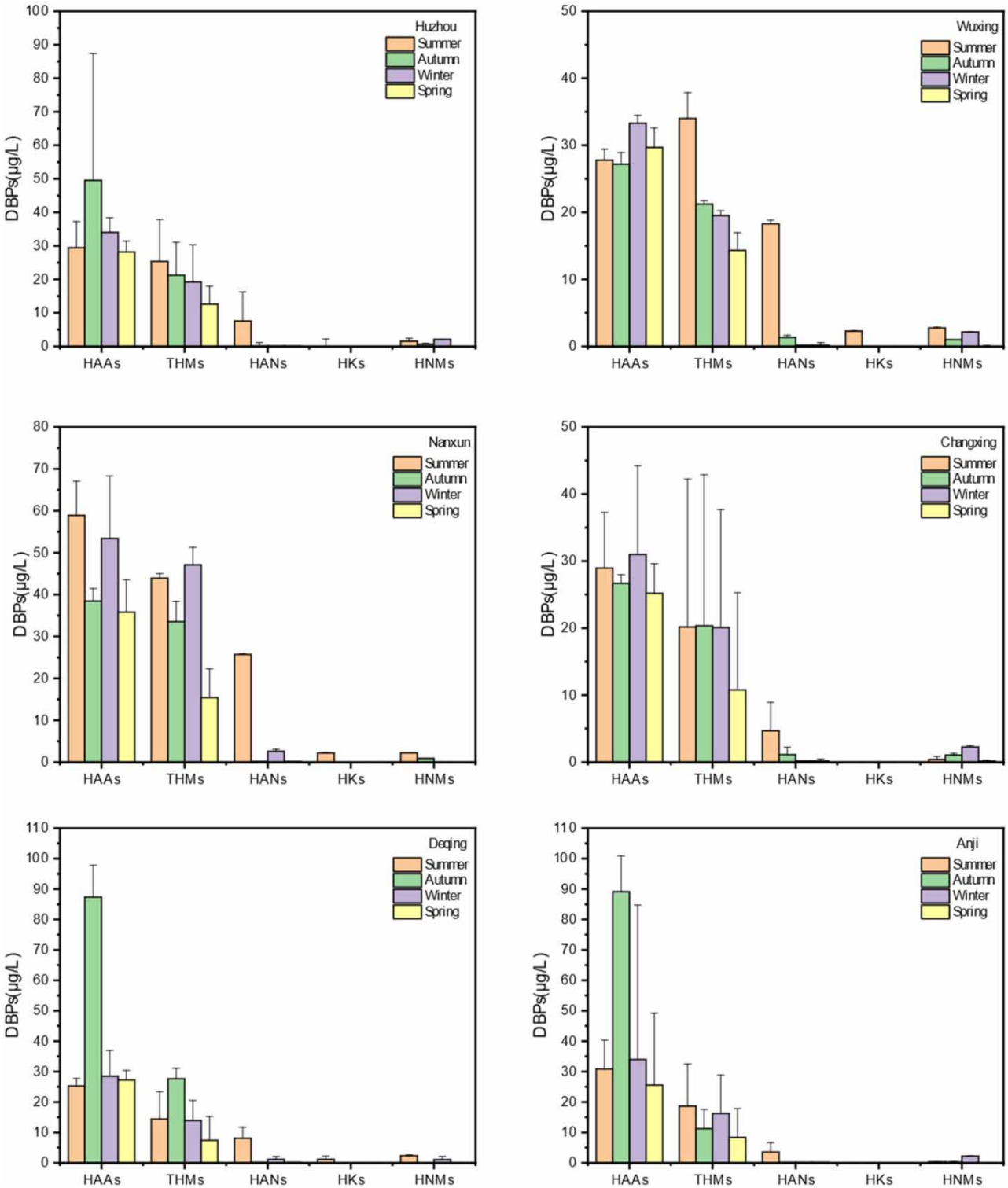

Figure 2 | Seasonal variation of DBPs in Huzhou's drinking water. (The top of the box shows median values, respectively; while the top of the whiskers shows the 75% of values, respectively).

increases with higher disinfectant dosage and residual chlorine (Zhang *et al.* 2017). Nanxun Water Plant sources its water from Taihu Lake, a body known for severe water pollution and rich organic matter content. Consequently, more DBPs are likely to be generated during chlorination and disinfection (Korotta-Gamage & Sathasivan 2017). Conversely, Anji

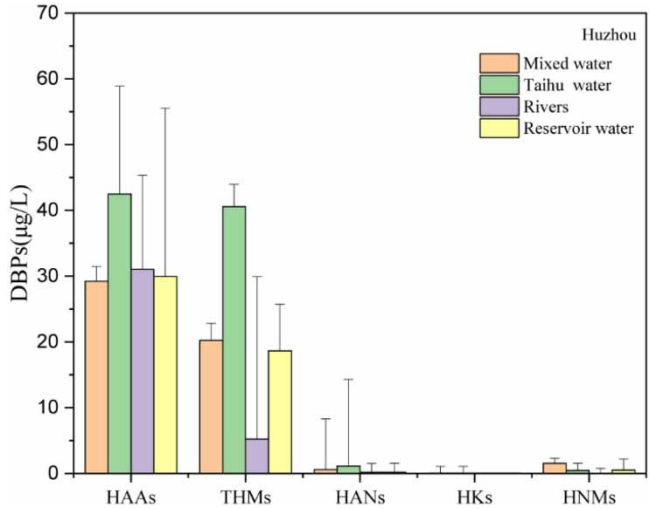

Figure 3 | Distribution of DBPs across diverse water sources in Huzhou's drinking water. (The top of the box shows median values, respectively; while the top of the whiskers shows the 75% of values, respectively).

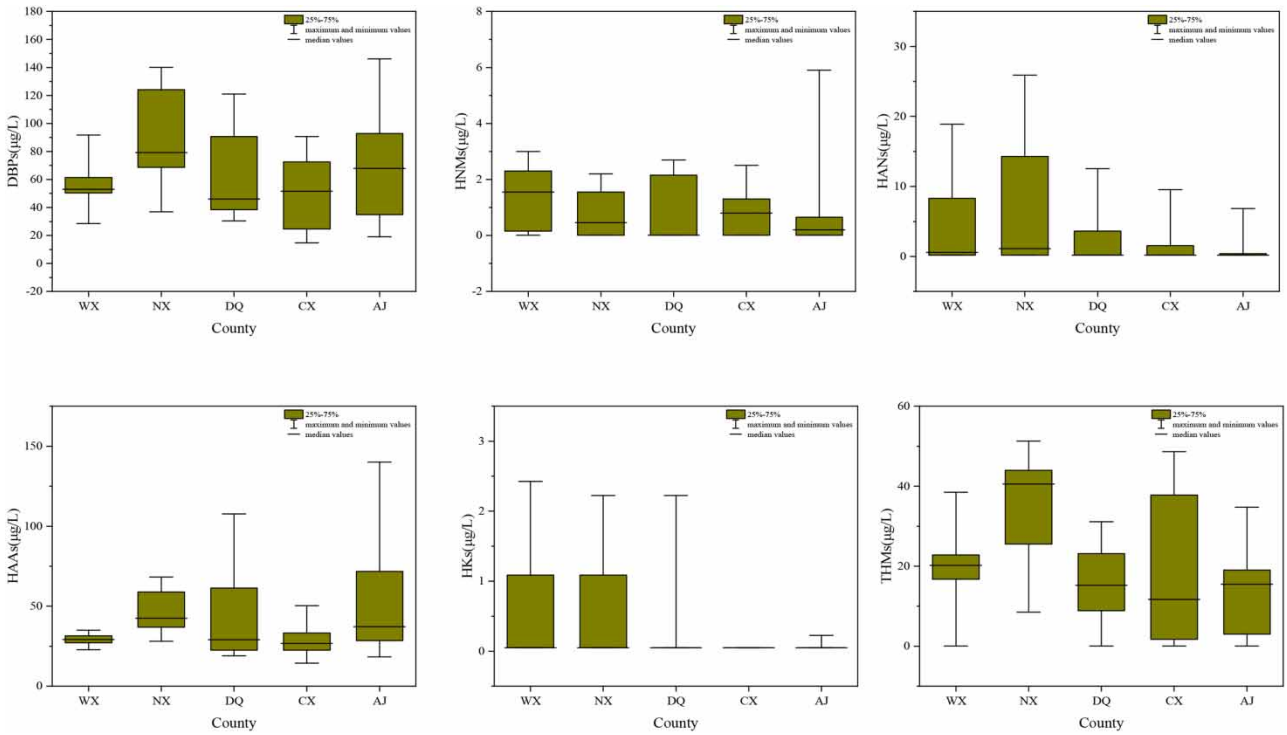

Figure 4 | Spatial distribution of DBPs in Huzhou's drinking water. (The bottom and top of the box show 25 and 75% of values. The top and bottom of the whiskers show the maximum and minimum values. The line across the box shows the median values.)

primarily uses reservoir water, which tends to elevate the DBPs in water plants more than river-sourced water (Padhi *et al.* 2019). HKs did not exhibit an apparent spatial distribution, possibly due to limited detection. The spatial distribution of HNMs diverged from other DBPs, reaching a maximum in Wuxing, followed by Changxing, while registering the lowest level in Deqing. As unstable DBPs, HNMs have a shorter existence in water and are known to hydrolyze at higher pH and temperature levels (Hong *et al.* 2013). In this study, Wuxing recorded the lowest pH and water temperature, at 6.65 and 17.0 °C, respectively, while Deqing had the highest values at pH 7.80 and 19.3 °C.

3.6. Relationship between DBPs concentration and water quality parameters

Table 5 demonstrates the relationship between each group of DBPs and specific water quality parameters. UV_{254} exhibited a significant negative correlation ($p < 0.05$) with HKs, while COD displayed a notable positive correlation ($p < 0.05$) with HANs. However, no discernable relationship was observed between COD or UV_{254} and other DBPs groups. Alterations in UV_{254} and COD typically induce changes in the generation and concentration of DBPs (Zhou *et al.* 2019). The removal of organics might explain the absence of a clear correlation between UV254, COD, and DBPs (Hong *et al.* 2015). The variance in organic matter removal rates across water plants in Huzhou possibly influences the formation of DBPs. Additionally, while UV254 and COD serve as indicators of organic matter in the water (Leziart *et al.* 2019), they lack the capability to discern whether such matter constitutes precursor compounds of DBPs (Ates *et al.* 2020).

Our study revealed a positive influence of temperature on the formation of HAAs, THMs, and HANs. These findings diverge slightly from those of Hong *et al.* (2013) and Yang *et al.* (2007). Several studies have documented that rising temperatures can catalyze DBP formation, as a warmer environment augments reaction rates. Conversely, elevated temperatures may impede the formation of unstable DBPs (such as HAAs, HANs, HKs) by accelerating their degradation rate (Chowdhury *et al.* 2011; Stefán *et al.* 2019). Thus, variations in temperature ranges can elicit either positive or negative shifts in DBP formation.

Apart from HNMs, our study found no significant correlation between pH and most DBPs, aligning with prior research (Zhou *et al.* 2019). This lack of notable association could be attributed to the comparable geographical environment and economic conditions of Huzhou and Jinhua, where variations in pH were relatively insignificant. Consequently, most DBPs did not exhibit a pronounced relationship with pH.

Turbidity demonstrated a substantial negative correlation ($p < 0.01$) with THMs, HANs, HKs, and HNMs. Turbidity is caused by a heterogeneous mixture encompassing various particle types and materials, including particles, colloids, and dissolved substances (Sillanpää *et al.* 2018). Notably, when these particles require chlorine, they can interfere with the chlorination disinfection process (Leziart *et al.* 2019), leading to a consequent reduction in the generation of DBPs.

The Cl^- demonstrated a significant ($p < 0.05$) positive association with most DBPs (HAAs, THMs, HANs). Concurrently, residual chlorine was found to correlate positively with HAAs, THMs, and HNMs. As the concentration of Cl^- and residual chlorine increases, the oxidation of organics in water samples is heightened, leading to an amplified formation of HAAs and THMs. This increase is directly proportional to the chlorine dose and reaction time (Zhang *et al.* 2017). However, it is worth noting that Cl^- and residual chlorine showed no significant relationship with HKs. This lack of correlation could be influenced by variables, such as pH, contact time, and overall water quality.

A principal component analysis was employed to investigate the potential factors influencing DBPs formation. The results revealed that four components explained 60.9% of the total variance (Table 6). The first component, with an initial eigenvalue of 3.084, accounted for 23.7% of the total variance, with significant loadings on HANs (0.898), HKs (0.885), HNMs (0.678), and THMs (0.589). This suggests that the first component represents the similar formation characteristics of these DBPs. The second component, with an initial eigenvalue of 1.716, accounted for 13.2% of the total variance and was significantly

Table 5 | The correlation between water quality parameters and DBPs in water samples

Parameters	HAAs	THMs	HANs	HKs	HNMs
UVA_{254}	−0.180	0.159	−0.069	−0.246*	0.075
pH	0.182	−0.051	−0.073	−0.130	−0.267*
Turbidity	−0.131	−0.463**	−0.367**	−0.385**	−0.471**
Cl^- (mg/L)	0.287**	0.403**	0.239*	0.162	0.134
Br^- (mg/L)	0.003	−0.065	0.000	0.000	0.000
COD (mg/L)	0.163	0.161	0.253*	0.216	0.177
Residue chlorine (mg/L)	0.325**	0.295**	0.093	0.105	0.254*
Temp (°C)	0.239*	0.311**	0.387**	0.203	0.195

r, Spearman correlation; *p*, sig (two-tailed).
**Significant at the 0.01 level (two-tailed).
*Significant at the 0.05 level (two-tailed).

Table 6 | Principal component analysis with varimax rotation for water quality parameters and DBPs in water samples

	Component			
	1	2	3	4
HANs	**0.898**	0.198	−0.023	0.087
HKs	**0.885**	0.092	−0.058	−0.013
HNMs	**0.678**	−0.122	0.209	−0.185
THMs	**0.589**	0.155	0.349	0.309
Temp (°C)	0.264	**0.835**	0.157	−0.125
COD (mg/L)	0.045	**0.828**	−0.156	−0.059
Residue chlorine (mg/L)	0.113	−0.125	**0.802**	−0.034
Turbidity	−0.282	−0.138	**− 0.619**	−0.081
HAAs	−0.230	**0.433**	**0.567**	0.181
UVA_{254}	0.008	0.043	−0.289	0.085
Cl^- (mg/L)	0.250	−0.127	0.060	**0.858**
Br^- (mg/L)	0.021	0.136	0.034	**− 0.608**
pH	−0.292	0.300	−0.132	**0.596**

The data were shown in bold form when more than 0.4, which indicates a good contribution of the variable to the component.

influenced by temperature (0.835), COD (0.828), and HAAs (0.433). This component suggests the profound role of temperature and organic matter in HAAs formation, thus influencing DBPs formation (Kim *et al.* 2017). The third component, having an initial eigenvalue of 1.676, explained 12.9% of the total variance. It was influenced by residual chlorine (0.802), turbidity (−0.619), and HAAs (0.567). This indicates that turbidity may impact the disinfection effect, signified by the consumption of chlorine and influenced HAAs formation. The fourth component, with an initial eigenvalue of 1.440, accounted for 11.1% of the total variance and was linked to Cl^- (0.858), Br^- (−0.608), and pH (0.596), which are fundamental constituents of water. During drinking water treatment procedures, the presence of Br^- and Cl^- significantly affected DBPs formation, and this process was pH-dependent.

4. CONCLUSION

This study examined the occurrence of 5 DBPs and relevant water quality parameters at 10 DWTPs of Huzhou. The results demonstrated that THMs and HAAs were the predominant DBPs across all samples, lower than those reported in Bushehr Province, Iran, Haihe River, China, and Nigeria, but higher than observations in Bohai Bay, China, and Indian river water. Seasonal variations indicated a similar trend in HAAs, THMs, HANs, and HNMs with concentrations in summer or autumn > spring. When considering water source variations, the levels of HAAs and THMs in Taihu water surpassed other sources. In a spatial context, the aggregate DBPs and HAAs levels were the highest in Nanxun, followed by Anji, while lower levels were found in Deqing and Changxing. The DBPs levels tended to increase with proximity to Taihu Lake. Correlation analysis between water quality parameters and DBPs indicated that chloride (Cl^-, in mg/L), temperature, and residual chlorine positively influenced the formation of DBPs, while turbidity exerted a negative effect. Principal component analysis further revealed that the formation characteristics of HANs, HKs, HNMs, and THMs were similar. Temperature, COD, and residual chlorine played crucial roles in the occurrence of HAAs, which might be associated with the pollution in Taihu and local climatic conditions. In conclusion, factors such as the formation and relations of HANs, HKs, HNMs, and THMs, organic matter content, chlorine consumption, and water constitution significantly contribute to the generation of DBPs.

ACKNOWLEDGEMENTS

This study was supported by the Zhejiang Province Public Technology Application Research Project (2016C37022), Zhejiang Province Public Technology Application Research Project (2016C33218), Zhejiang Province Medical and Health Science and Technology Project (2018RC072), Huzhou Science and Technology Project (2018GYB03), Key Laboratory of Emergency detection for Public Health of Huzhou. Key Supporting Discipline of Huzhou Medical.

DATA AVAILABILITY STATEMENT

All relevant data are included in the paper or its Supplementary Information.

CONFLICT OF INTEREST

The authors declare there is no conflict.

REFERENCES

Abbas, S., Hashmi, I., Rehman, M. S. U., Qazi, I. A., Awan, M. A. & Nasir, H. 2014 Monitoring of chlorination disinfection by-products and their associated health risks in drinking water of Pakistan. *J. Water Health* **13** (1), 270–284. https://doi.org/10.2166/wh.2014.096.

Ates, N., Kaplan-Bekaroglu, S. S. & Dadaser-Celik, F. 2020 Spatial/temporal distribution and multi-pathway cancer risk assessment of trihalomethanes in low TOC and high bromide groundwater. *Environ. Sci. Processes Impacts* **22** (11), 2276–2290.

Benson, N. U., Akintokun, O. A. & Adedapo, A. E. 2017 Disinfection byproducts in drinking water and evaluation of potential health risks of long-term exposure in Nigeria. *J. Environ. Public Health* **2017**, 1–10.

Charisiadis, P., Andra, S. S., Makris, K. C., Christophi, C. A., Skarlatos, D., Vamvakousis, V., Kargaki, S. & Stephanou, E. G. 2015 Spatial and seasonal variability of tap water disinfection by-products within distribution pipe networks. *Sci. Total Environ.* **506–507**, 26–35.

Chowdhury, S. 2018 Disinfection by-products in desalinated and blend water: formation and control strategy. *J. Water Health* **17** (1), 1–24.

Chowdhury, S., Rodriguez, M. J. & Sadiq, R. 2011 Disinfection byproducts in Canadian provinces: associated cancer risks and medical expenses. *J. Hazard. Mater.* **187** (1), 574–584.

Dobaradaran, S., Shabankareh Fard, E., Tekle-Röttering, A., Keshtkar, M., Karbasdehi, V. N., Abtahi, M., Gholamnia, R. & Saeedi, R. 2020 Age-sex specific and cause-specific health risk and burden of disease induced by exposure to trihalomethanes (THMs) and haloacetic acids (HAAs) from drinking water: an assessment in four urban communities of Bushehr Province, Iran, 2017. *Environ. Res.* **182**, 109062.

Fang, J., Ma, J., Yang, X. & Shang, C. 2010 Formation of carbonaceous and nitrogenous disinfection by-products from the chlorination of *Microcystis aeruginosa*. *Water Res.* **44** (6), 1934–1940.

Hao, R., Zhang, Y., Du, T., Yang, L., Adeleye, A. S. & Li, Y. 2017 Effect of water chemistry on disinfection by-product formation in the complex surface water system. *Chemosphere* **172**, 384–391.

Hong, H., Xiong, Y., Ruan, M., Liao, F., Lin, H. & Liang, Y. 2013 Factors affecting THMs, HAAs and HNMs formation of Jin Lan Reservoir water exposed to chlorine and monochloramine. *Sci. Total Environ.* **444**, 196–204.

Hong, H., Qian, L., Xiong, Y., Xiao, Z., Lin, H. & Yu, H. 2015 Use of multiple regression models to evaluate the formation of halonitromethane via chlorination/chloramination of water from Tai Lake and the Qiantang River, China. *Chemosphere* **119**, 540–546.

Hrudey, S. E., Backer, L. C., Humpage, A. R., Krasner, S. W., Michaud, D. S., Moore, L. E., Singer, P. C. & Stanford, B. D. 2015 Evaluating evidence for association of human bladder cancer with drinking-water chlorination disinfection by-products. *J. Toxicol. Environ. Health, Part B* **18** (5), 213–241.

Jeong, C. H., Postigo, C., Richardson, S. D., Simmons, J. E., Kimura, S. Y., Mariñas, B. J., Barcelo, D., Liang, P., Wagner, E. D. & Plewa, M. J. 2015 Occurrence and comparative toxicity of haloacetaldehyde disinfection byproducts in drinking water. *Environ. Sci. Technol.* **49** (23), 13749–13759.

Jiang, J., Han, J. & Zhang, X. 2020 Nonhalogenated aromatic DBPs in drinking water chlorination: a gap between NOM and halogenated aromatic DBPs. *Environ. Sci. Technol.* **54** (3), 1646–1656.

Kali, S., Khan, M., Ghaffar, M. S., Rasheed, S., Waseem, A., Iqbal, M. M., Bilal Khan Niazi, M. & Zafar, M. I. 2021 Occurrence, influencing factors, toxicity, regulations, and abatement approaches for disinfection by-products in chlorinated drinking water: a comprehensive review. *Environ. Pollut.* **281**, 116950.

Kim, D., Ates, N., Bekaroglu, S. S. K., Selbes, M. & Karanfil, T. 2017 Impact of combining chlorine dioxide and chlorine on DBP formation in simulated indoor swimming pools. *J. Environ. Sci.* **58**, 155–162.

Kolb, C., Francis, R. A. & VanBriesen, J. M. 2017 Disinfection byproduct regulatory compliance surrogates and bromide-associated risk. *J. Environ. Sci.* **58**, 191–207.

Korotta-Gamage, S. M. & Sathasivan, A. 2017 A review: potential and challenges of biologically activated carbon to remove natural organic matter in drinking water purification process. *Chemosphere* **167**, 120–138.

Kumari, M., Gupta, S. K. & Mishra, B. K. 2015 Multi-exposure cancer and non-cancer risk assessment of trihalomethanes in drinking water supplies – a case study of Eastern region of India. *Ecotoxicol. Environ. Saf.* **113**, 433–438.

Leziart, T., Dutheil, P. M., Cheswick, R., Jarvis, P. & Nocker, A. J. E. T. 2019 Effect of turbidity on water disinfection by chlorination with the emphasis on humic acids and chalk. *Environ. Technol.* **40** (13–16), 1–24.

Ly, Q. V., Maqbool, T. & Hur, J. 2017 Unique characteristics of algal dissolved organic matter and their association with membrane fouling behavior: a review. *Environ. Sci. Pollut. Res.* **24** (12), 11192–11205.

Mao, Y.-Q., Wang, X.-M., Guo, X.-F., Yang, H.-W. & Xie, Y. F. 2016 Characterization of haloacetaldehyde and trihalomethane formation potentials during drinking water treatment. *Chemosphere* **159**, 378–384.

MOH 2006 *Hygienic Standard for Drinking Water in People's Republic of China (GB 5749-2006)*.

Mompremier, R., Fuentes Mariles, Ó. A., Becerril Bravo, J. E. & Ghebremichael, K. 2018 Study of the variation of haloacetic acids in a simulated water distribution network. *Water Supply* **19** (1), 88–96.

Niu, Z., Li, X. & Zhang, Y. 2017 Composition profiles, levels, distributions and ecological risk assessments of trihalomethanes in surface water from a typical estuary of Bohai Bay, China. *Mar. Pollut. Bull.* **117** (1), 124–130.

Padhi, R. K., Subramanian, S. & Satpathy, K. K. 2019 Formation, distribution, and speciation of DBPs (THMs, HAAs, ClO_2^-, and ClO_3^-) during treatment of different source water with chlorine and chlorine dioxide. *Chemosphere* **218**, 540–550.

Sillanpää, M., Ncibi, M. C., Matilainen, A. & Vepsäläinen, M. 2018 Removal of natural organic matter in drinking water treatment by coagulation: a comprehensive review. *Chemosphere* **190**, 54–71.

Stefán, D., Erdélyi, N., Izsák, B., Záray, G. & Vargha, M. 2019 Formation of chlorination by-products in drinking water treatment plants using breakpoint chlorination. *Microchem. J.* **149**, 104008.

USEPA. 2010 *Comprehensive Disinfectants and Disinfection Byproducts Rules (Stage 1 and Stage 2): Quick Reference Guide*. pp. EPA 816-F-810-080.

Wang, Y., Zhu, G. & Engel, B. 2019 Health risk assessment of trihalomethanes in water treatment plants in Jiangsu Province, China. *Ecotoxicol. Environ. Saf.* **170**, 346–354.

Wei, J., Ye, B., Wang, W., Yang, L., Tao, J. & Hang, Z. 2010 Spatial and temporal evaluations of disinfection by-products in drinking water distribution systems in Beijing, China. *Sci. Total Environ.* **408** (20), 4600–4606.

WHO 2004 *Guidelines for Drinking-Water Quality*, 3rd edn. World Health Organization, Geneva.

Wu, Z., Wang, X., Chen, Y., Cai, Y. & Deng, J. 2018 Assessing river water quality using water quality index in Lake Taihu Basin, China. *Sci. Total Environ.* **612**, 914–922.

Wu, T., Zhu, G., Zhu, M., Xu, H. & Zhang, Y. 2020 Use of conductivity to indicate long-term changes in pollution processes in Lake Taihu, a large shallow lake. *Environ. Sci. Pollut. Res.* **27** (17), 21376–21385.

Yang, M. & Zhang, X. 2016 Current trends in the analysis and identification of emerging disinfection byproducts. *Trends Environ. Anal. Chem.* **10**, 24–34.

Yang, X., Shang, C. & Westerhoff, P. 2007 Factors affecting formation of haloacetonitriles, haloketones, chloropicrin and cyanogen halides during chloramination. *Water Res.* **41** (6), 1193–1200.

Zhang, Y., Chu, W., Yao, D. & Yin, D. 2017 Control of aliphatic halogenated DBP precursors with multiple drinking water treatment processes: formation potential and integrated toxicity. *J. Environ. Sci.* **58**, 322–330.

Zheng, J., Su, C., Zhou, J., Xu, L., Qian, Y. & Chen, H. 2017 Effects and mechanisms of ultraviolet, chlorination, and ozone disinfection on antibiotic resistance genes in secondary effluents of municipal wastewater treatment plants. *Chem. Eng. J.* **317**, 309–316.

Zhou, X., Zheng, L., Chen, S., Du, H., Gakoko Raphael, B. M., Song, Q., Wu, F., Chen, J., Lin, H. & Hong, H. 2019 Factors influencing DBPs occurrence in tap water of Jinhua Region in Zhejiang Province, China. *Ecotoxicol. Environ. Saf.* **171**, 813–822.

First received 9 May 2023; accepted in revised form 23 August 2023. Available online 22 September 2023